Comparison of Pressure-Swing Distillation and Extractive Distillation Methods for Isopropyl Alcohol/Diisopropyl Ether Separation

ARTICLE *in* INDUSTRIAL & ENGINEERING CHEMISTRY RESEARCH · OCTOBER 2014

Impact Factor: 2.59 · DOI: 10.1021/ie502735g

6 AUTHORS, INCLUDING:

Li Weisong
Tianjin University
9 PUBLICATIONS **41** CITATIONS

SEE PROFILE

I&EC research
Industrial & Engineering Chemistry Research

Article

pubs.acs.org/IECR

Comparison of Pressure-Swing Distillation and Extractive Distillation Methods for Isopropyl Alcohol/Diisopropyl Ether Separation

Haotao Luo, Kai Liang, Weisong Li, Ye Li, Ming Xia, and Chunjian Xu*

State Key Laboratory of Chemical Engineering, Chemical Engineering Research Center, and School of Chemical Engineering and Technology, Tianjin University, Tianjin 300072, China

ABSTRACT: In the production of isopropyl alcohol, diisopropyl ether appears as a byproduct. Diisopropyl ether and isopropyl alcohol form a binary minimum-boiling homogeneous azeotrope. In this paper, two methods are explored to achieve the separation of this binary azeotrope: fully heat-integrated pressure-swing distillation and extractive distillation with 2-methoxyethanol as an entrainer. The optimal design and dynamic control of the two processes are investigated, respectively. It is revealed that the fully heat-integrated pressure-swing distillation system offers 5.75% reduction in the total annual cost and 7.97% saving in energy consumption as compared to the extractive distillation system. Moreover, control configurations of both processes performed nicely in maintaining the two products' quality when feed flow rate and composition disturbances are introduced. From the standpoint of dynamic control stability, both processes can be used for DIPE/IPA separation.

1. INTRODUCTION

Diisopropyl ether (DIPE) is a widely used chemical in many different fields, such as fossil oil, tobacco production, and synthetic chemistry. Specifically, it is used as a specialized solvent to remove polar organic compounds from aqueous solutions, for example, phenols, ethanol, acetic acid, whereas isopropyl alcohol (IPA) mainly finds its use in medicine industry as a chemical intermediate and solvent.[1,2]

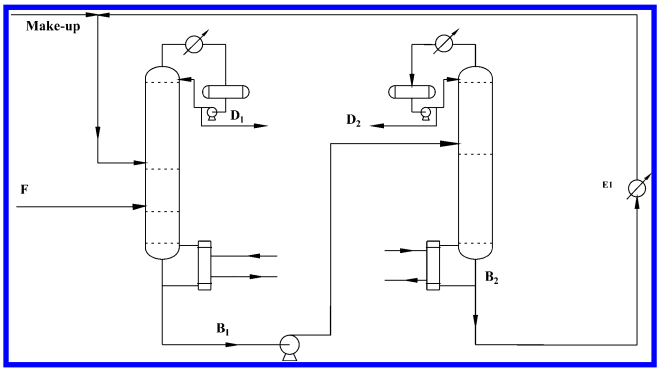

Figure 1. Sketch of the extractive distillation process.

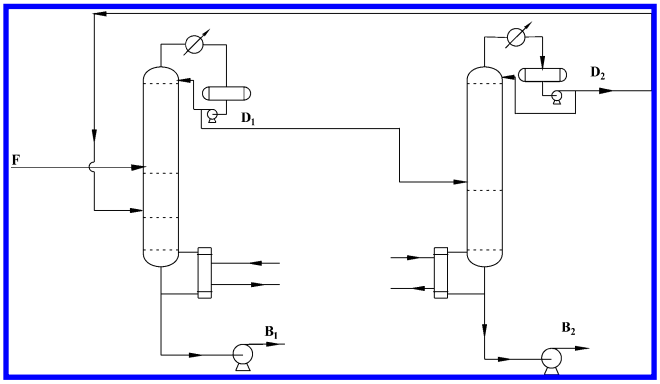

Figure 2. Sketch of pressure-swing distillation process.

IPA is produced by using solid acid or liquid acid as catalytic agent, with DIPE as a coproduct.[2] The separation of DIPE/IPA is the key downstream process that determines the entire process economic benefits. Since IPA and DIPE form a binary minimum-boiling homogeneous azeotrope, conventional distillation methods cannot achieve this separation effectively. Hence, other types of distillation methods are necessary for this separation.

Extractive distillation commonly finds its application in the separation of binary azeotropes and other mixtures with the relative volatilities of key components below 1.1.[3−7] Because entrainer interacts differently with the two components of a binary azeotrope, it increases the relative volatility of both the light and heavy components. For extractive distillation system, as shown in Figure 1, two high-purity products are obtained at the tops of two columns with the entrainer being recovered at the bottoms of the entrainer recovery column. Then, entrainer is recycled to the extractive distillation column.[8] Lang investigated extractive distillation methods to the separation of maximum boiling azeotropes with continuous entrainer feeding.[9,10] Lei et al. explored salt-addition distillation methods to separate azeotropes.[11] Chien and co-workers studied extractive distillation systems for the separation of water and IPA.[12] Wang et al. explored the extractive distillation system for methylal/methanol separation.[13] Knapp and Doherty investigated the heat integration of extractive distillation methods for binary homogeneous azeotropic systems.[14]

Some azeotropic systems exhibit the property that the azeotropic compositions change significantly with pressure, in this circumstance pressure-swing distillation can be used. As seen

Received: July 9, 2014
Revised: August 26, 2014
Accepted: September 4, 2014
Published: September 4, 2014

dx.doi.org/10.1021/ie502735g | Ind. Eng. Chem. Res. 2014, 53, 15167−15182

in Figure 2, with two columns operating at different pressures, two high-purity products are obtained in the bottoms of two columns. Lewis appears to be the first to recommend pressure-swing distillation for the separation of an azeotrope.[15] Müller investigated pressure-swing distillation for the separation of methanol/methylal mixtures.[16] Muñoz explored pressure-swing distillation methods for the separation of isobutyl alcohol and isobutyl acetate.[17] Luyben studied a heat-integrated pressure-swing distillation system for the separation of acetone and methanol.[18]

Effective control structure ensuring a robust dynamic performance for a chemical process is the other important aspect for distillation systems. Skogestad reviewed distillation columns dynamics and control in detail, highlighting advances in distillation process control in the past few decades.[19] On this issue, appropriate controlled variables and manipulated variables are selected for establishing distillation control systems. Luyben used the relative gain array (RGA) for the pairing of controlled variables and manipulated variables.[20] Composition control and temperature control are commonly used for controlling extractive distillation and pressure-swing distillation. Composition control brings in long drag time and is costly in both equipment and maintenance. Therefore, temperature control is more widely used in distillation. Luyben studied temperature control structure of extractive distillation for the separation of TAME/methanol, with one temperature controlled for each column by manipulating the corresponding reboiler heat input.[21] Wang[13] et al. explored the temperature control structure of an extractive distillation system for methylal/methanol separation. It was found that the structure with the ratio of reflux flow rate/feed flow rate (R/F) schemes gave good dynamic responses. Furthermore, Yu[22] investigated temperature control for fully heat-integrated pressure-swing distillation and revealed that the pressure-compensated temperature control structure offered fairly good dynamic responses.

The purity of the product IPA or DIPE has great influence on the economic benefit; thus separation of this binary minimum-boiling homogeneous azeotrope is of significance. Pressure-swing distillation and extractive distillation have been discussed,[23,24] but the literature on the separation of IPA/DIPE mixture via the above-mentioned methods is rather limited. Therefore, it is desirable to explore feasible distillation systems for this mixture separation, with emphasis on achievement of the optimum economic design and establishment of the effective control strategy.

In this work, two special distillation systems are investigated for the separation of DIPE/IPA: fully heat-integrated pressure-swing distillation and extractive distillation systems. First, on the basis of the total annual costs (TAC), the optimized configurations of two distillation systems are attained with the proposed global optimization procedures. Moreover, effective control structures are explored for the extractive distillation control system and pressure-swing distillation control system. Finally, steady-state and dynamic comparisons between the fully heat-integrated pressure-swing distillation process and extractive distillation process are also made for this azeotropic separation.

2. STEADY STATE DESIGN

2.1. Extractive Distillation. *2.1.1. Entrainer Selection.* Since entrainer plays an important role in extractive distillation, attention should be paid to its selection. A criterion for entrainer selection is the comparison of the relative volatilities in the presence of different entrainers.[25] The higher the relative volatility, the easier the separation. Of all entrainer candidates used for the separation of the IPA and DIPE azeotrope mixture, the following three entrainers are studied in this work: 3-methyl-1-butanol,[26] 2-methoxyethanol,[27] and 1-methoxy-2-propanol.[28] Their bubble point (T_b) and the relative volatility ($\alpha^S_{1,2}$, the relative volatility of DIPE and IPA in the presence of entrainer S) are listed in Table 1. Because 2-methoxyethanol (2-MEA) does not bring in further azeotropes in the system and shows a higher relative volatility (2.30), it is chosen as the entrainer in the simulation.

Table 1. Results of the Entrainer Selection for Extractive Distillation System

DIPE (1)/IPA (2) using the NRTL model		
entrainer (100.00 wt %)	T_b/K	$\alpha^S_{1,2}$
2-methoxyethanol	397.67	2.30
1-methoxy-2-propanol	393.24	1.77
3-methyl-1-butanol	404.16	1.41

Table 2. Regressed Binary Interaction Parameters for the Aspen Plus NRTL Model

	DIPE(i)/IPA(j)	DIPE(i)/2-MEA (j)	IPA(i)/2-MEA (j)
A_{ij}	−1.644	−7.773	−3.157
A_{ji}	−1.508	5.377	−1.274
B_{ij}/K	709.543	3123.789	1433.818
B_{ji}/K	772.315	−1672.885	248.282
C_{ij}	0.300	0.300	0.300

2.1.2. Thermodynamic Model and Feasibility Analysis. In this study, the NRTL model is used to describe the nonideality of the liquid phase, while the vapor phase is assumed to be ideal. The binary interaction parameters of the three pairs are regressed with the experimental data,[27] and all other physical property parameters are taken from the built-in values in Aspen Plus. Their binary interaction parameters are listed in Table 2. The predicted azeotropic composition and azeotropic temperature for DIPE (1)/IPA (2) at 1 atm are 77.01/22.99 mol % DIPE/IPA and 339.97 K, respectively.

The design and synthesis of an azeotropic distillation process with RCM were investigated by Doherty.[29,30] A residue curve map (RCM) can be used as a simple method for designing and distinguishing between feasible and infeasible sequences for a given system. The RCM of the DIPE/IPA/2-MEA ternary system mapped by Aspen Plus using the NRTL model is shown in Figure 4. It is observed that both DIPE and IPA are the saddles, 2-MEA is the stable node, and the DIPE/IPA azeotrope is the unstable node. The resulting residue curves (brownness lines) with arrows point to pure 2-MEA. Also, we can find no presence of the distillation boundary. This is an ideal situation for selection of an extractive distillation process. The blue line stands for the material balance line. It is noticed that F_1 is separated into D_1 and B_1, and B_1 is separated into D_2 and B_2. This means that the entrainer helps the feed to be separated into fairly pure products. To balance the tiny loss of entrainer in both D_1 and D_2 streams, a small makeup stream of 2-MEA should be added.

2.1.3. Process Design and Economic Analysis. In this work, the composition of the raw material composition is close to the azeotropic composition regardless of the preconcentration columns. Therefore, the distillation system consists of two columns: extractive distillation column and entrainer recovery column. The extractive distillation process was simulated with the following data: the feed mixture consists of 75/25 mol %

dx.doi.org/10.1021/ie502735g | Ind. Eng. Chem. Res. 2014, 53, 15167−15182

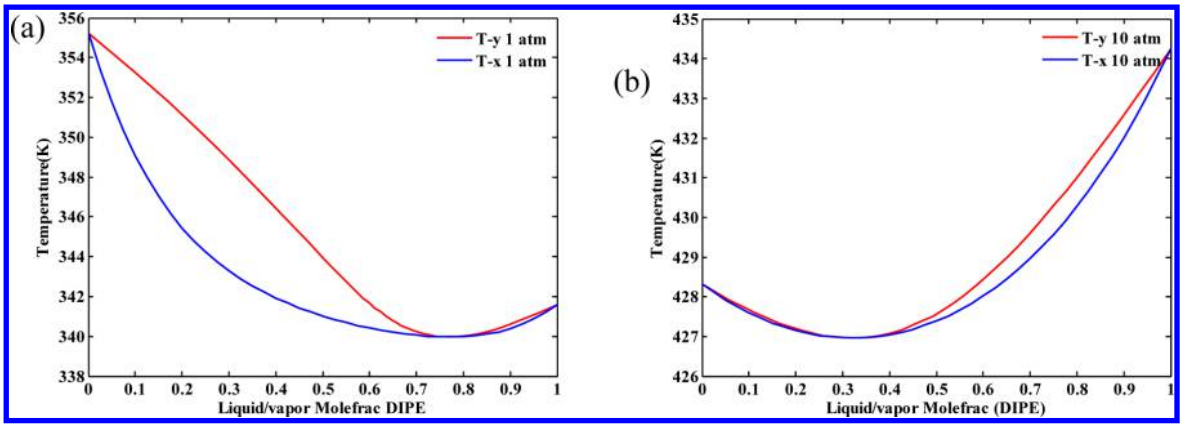

Figure 3. $T-x,y$ diagram for DIPE/IPA at (a) 1 atm and (b) 10 atm.

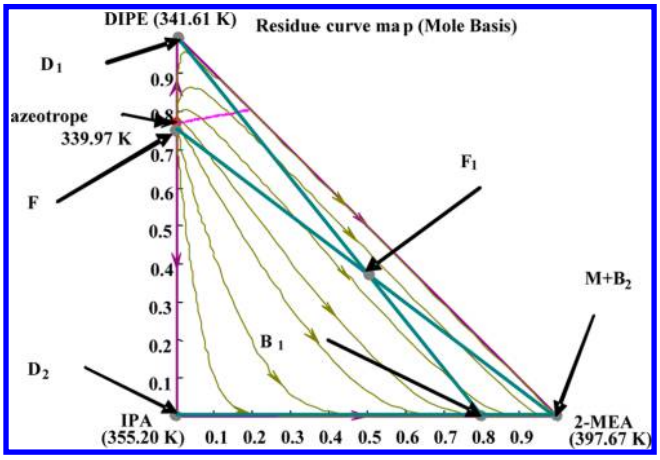

Figure 4. Residue curve map at 1 atm for the DIPE/IPA/2-MEA system.

DIPE/IPA, with a flow rate of 100 kmol/h. The two product specifications are set to be as follows: the DIPE and IPA products have a purity of 99.5 wt %. The condenser pressures of both the extractive distillation column and the entrainer recovery column are set at 1 atm with an assumed tray pressure drop of 0.0068 atm. The steady state design is implemented by commercial software (Aspen Plus). Useful skills on how to use these software programs are covered in detail in Lyuben's book.[31]

We use Aspen notation of numbering stages from the top, with stage 1 being the reflux drum and the last stage being the rebolier. For an extractive distillation column, there are three design degrees of freedom once the total stages, operating pressure, and feed location are fixed: reflux ratio (RR_1), entrainer flow rate (S), and reboiler heat duty (QR_1). Before the rigorous simulation of steady state, several case studies are made to investigate the influence of the flow rate of entrainer and reflux ratio on the product composition. In each case, the number of theoretical plates (N_{T1}) is fixed. Figure 5 shows the influence of S and RR_1 on the compositions of the distillate stream from the extractive distillation column with N_{T1} = 66, N_{FE} = 56, N_{F1} = 30.

Figure 5a shows that for a given entrainer flow rate, S, there is an optimum reflux ratio, RR_1, that gives the maximum DIPE purity. The higher is the entrainer flow rate, the higher is the DIPE purity that could be obtained. To achieve the desired 99.5

Table 3. Basis of Economics

condensers	heat-transfer coefficient = 0.852 kW/K·m^2
	capital cost = $7296A_C^{0.65}$($) where area is in squared meters
reboilers	heat-transfer coefficient = 0.568 kW/K·m^2
	capital cost = $7296A_R^{0.65}$($) where area is in squared meters
column vessel	capital cost = $17640D^{1.066}L^{0.802}$($) where D and L are in meters
	payback period = 3 annum

Table 4. Utility Prices

utility	price ($/GJ)
high pressure steam (41 barg)	17.7
medium pressure steam (10 barg)	14.19
low pressure steam (5 barg)	13.28
cooling water	0.354

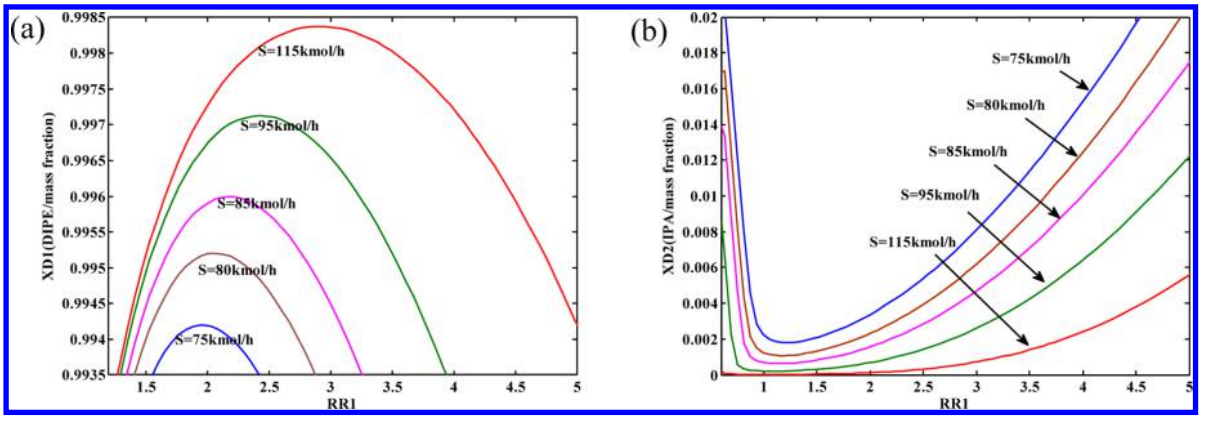

Figure 5. Effect of RR_1 and entrainer flow rate S in the extractive column (N_{T1} = 66, N_{FE} = 56, N_{F1} = 30) on (a) DIPE purity and (b) impurity of IPA.

dx.doi.org/10.1021/ie502735g | Ind. Eng. Chem. Res. 2014, 53, 15167−15182

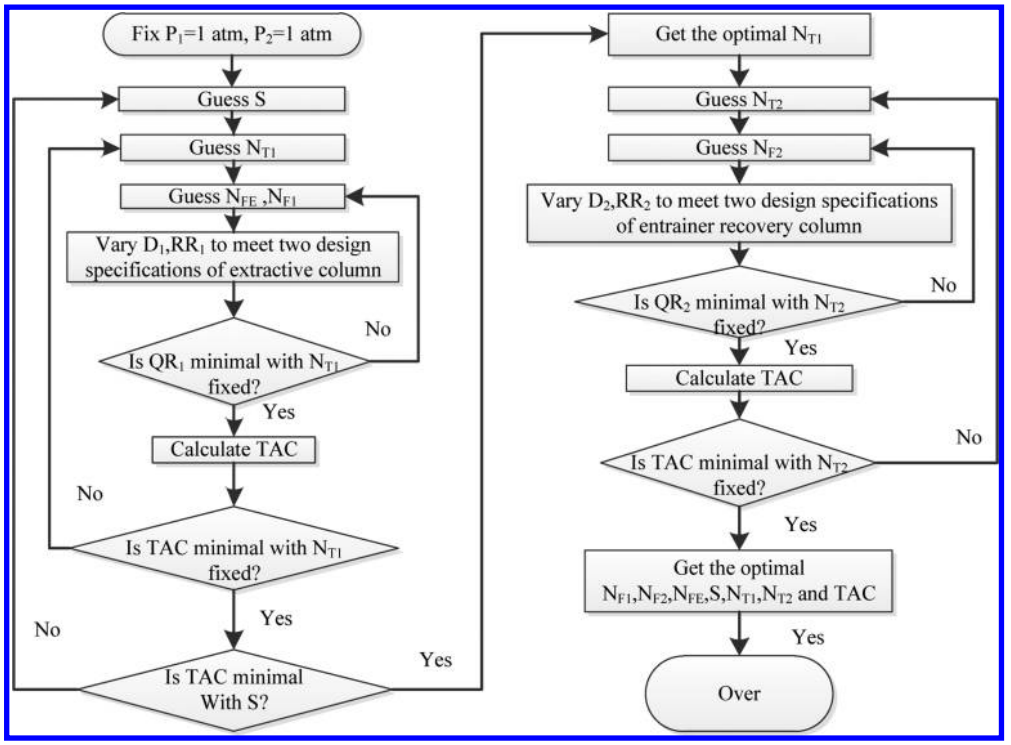

Figure 6. Sequential iterative optimization procedure for the conventional extractive distillation system.

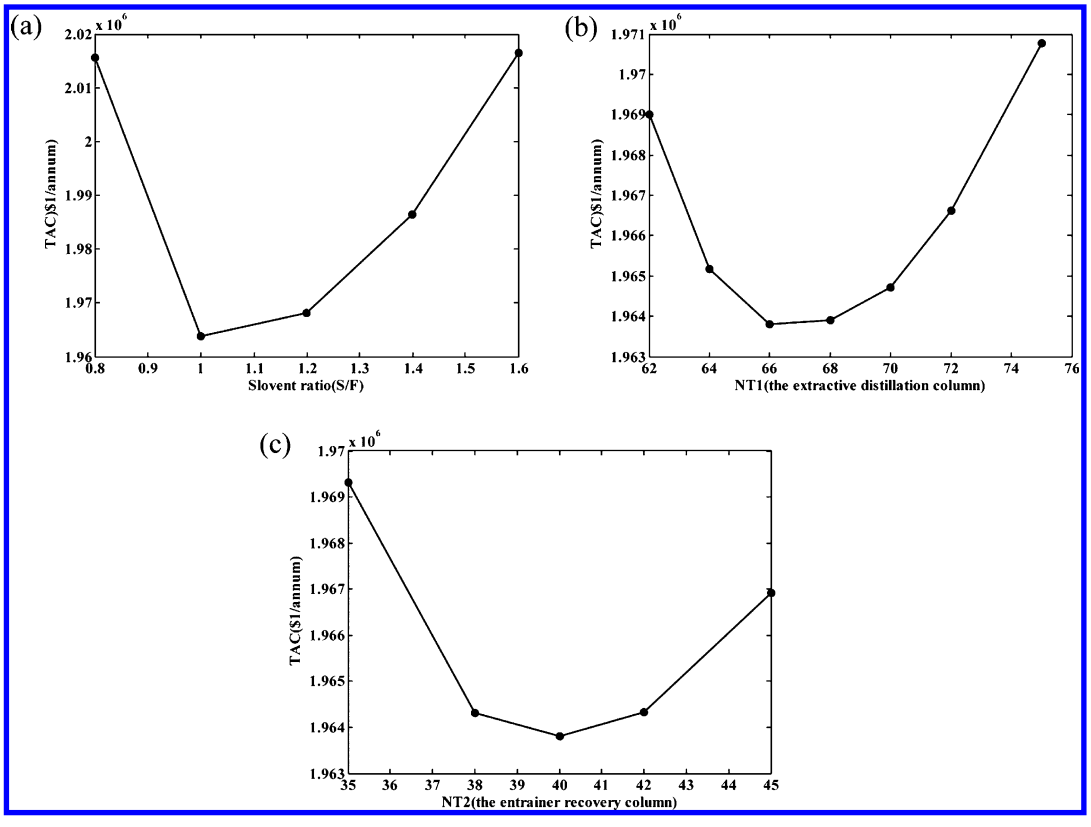

Figure 7. TAC vs (a) *S*/*F* ratio (mole), stages for (b) the extractive distillation column (c) entrainer recovery column.

wt % DIPE purity, the entrainer flow rate must exceed 80 kmol/h at a reflux ratio of about 2. Figure 5b shows how the impurity of IPA in D_1 is affected by entrainer flow rate and reflux ratio.

As mentioned above, the influences of the flow rate of entrainer and reflux ratio on the product composition are investigated. Then, the rigorous simulation of steady state is implemented by using the "RadFrac" block. These runs are made with the distillate and bottoms compositions held at their specified values. In the extractive distillation column, the composition ratio of DIPE and IPA in the bottoms is 0.0049,

dx.doi.org/10.1021/ie502735g | *Ind. Eng. Chem. Res.* 2014, 53, 15167−15182

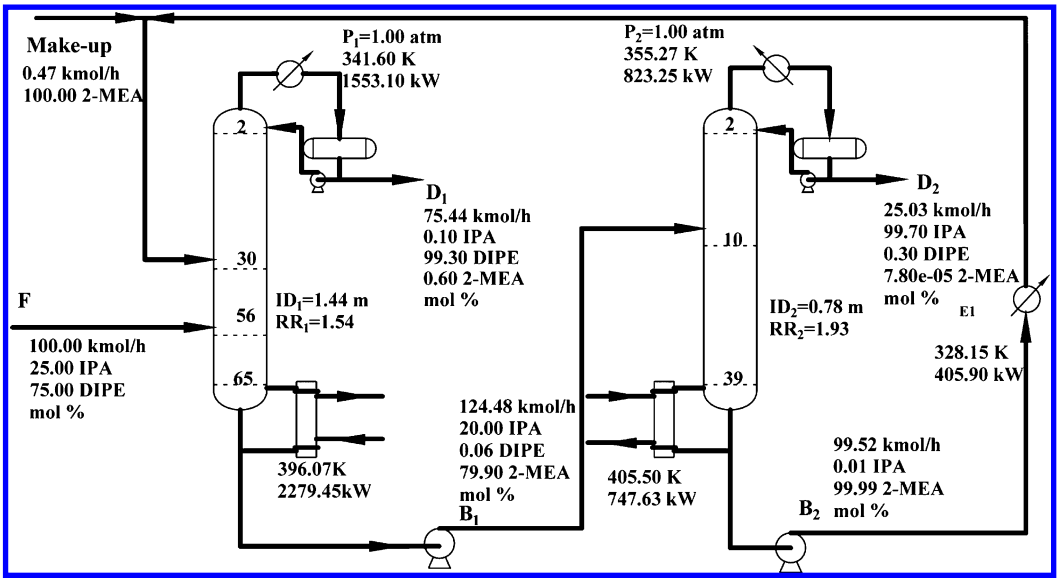

Figure 8. Optimal flowsheet for the conventional extractive distillation system.

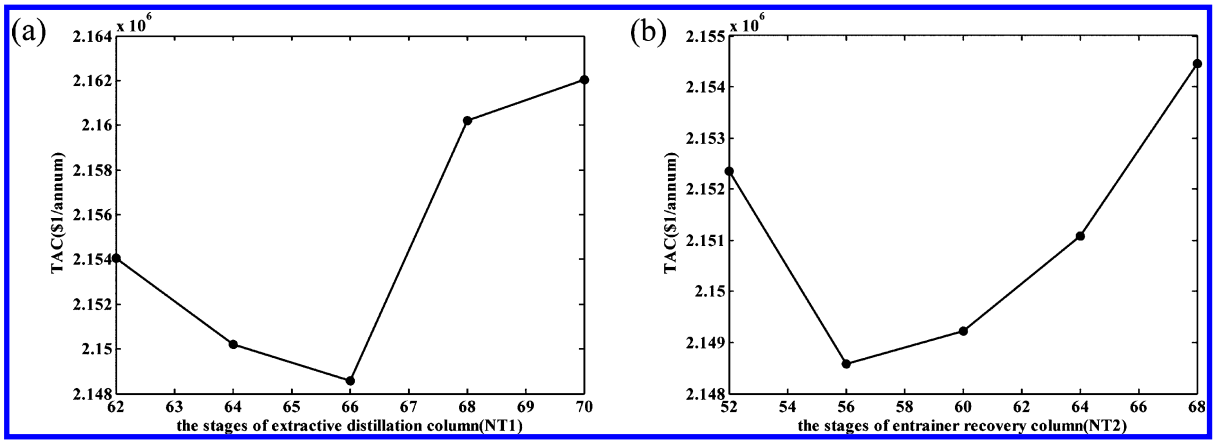

Figure 9. TAC vs stages of (a) extractive distillation column and (b) entrainer recovery column.

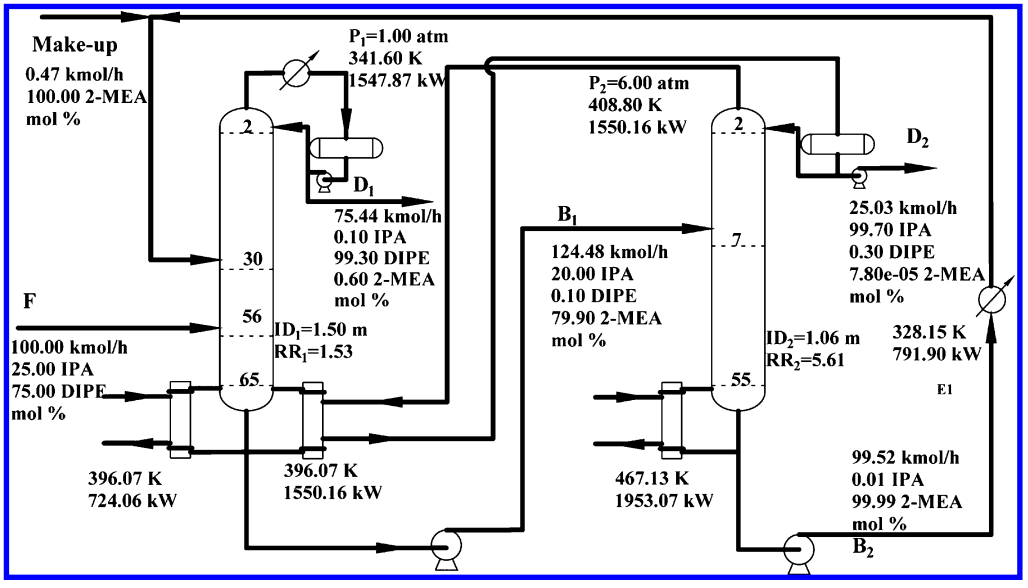

Figure 10. Optimal flowsheet for the partially heat-integrated extractive distillation system.

and the distillate composition specification is 99.5 wt % DIPE. In the entrainer recovery column, the bottoms composition specification is 10^{-5} wt % IPA and the distillate composition specification is 99.5 wt % IPA. The entrainer feed temperature is

dx.doi.org/10.1021/ie502735g | Ind. Eng. Chem. Res. 2014, 53, 15167−15182

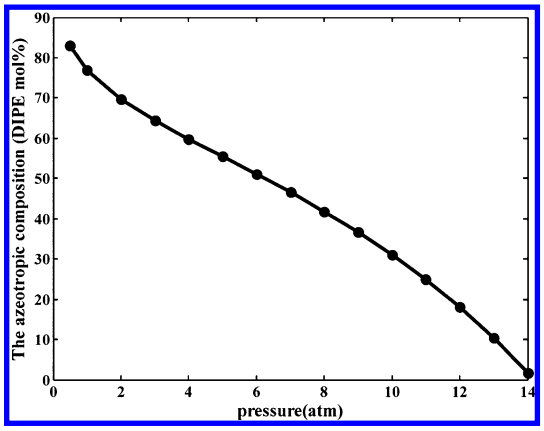

Figure 11. Effect of pressure on azeotropic composition.

also a process design variable, thus, a cooler is required. Knight and Doherty[32] advised that the entrainer feed temperature should be 5 to 15 K below the top temperature of the extractive distillation column, the entrainer feed temperature is fixed at 328.15 K in the simulations.

Total annual cost (TAC) is adopted as the objective function to be minimized by adjusting the design parameters, including the number of trays in each column, the feed location in the column, etc. The TAC is defined as[33]

$$\mathrm{TAC} = C_V + 0.3\mathrm{FCI} \quad (1)$$

where the C_V is the process variable costs, mostly utilities consumption (steam, cooling water, and electricity); FCI is the fixed capital investment.

Because the cost of the entrainer ($\$0.00192 \times 10^6$/annum) is much lower than the minimum TACs of two processes ($\$1.9638 \times 10^6$ and 1.85091×10^6/annum), the cost of the entrainer is ignored. The major pieces of equipment for the DIPE/IPA separation process are the two column vessels, two reboilers, and two condensers. Other items such as pipes, valves, pumps, and the reflux drums are usually not considered, because their costs are usually much less than the costs of the vessels and heat exchangers. Since the two columns have small diameters, we specify the tray spacing to be 0.4 m instead of the default value (0.61 m) in the simulator, and a sieve plate is selected. The heat transfer areas for the condenser and reboiler are calculated by the heat duty, the overall heat transfer coefficient, and the differential temperature driving force. The economic parameter values and the sizing relationships and parameters used in this work are given in Tables 3 and 4,[18,31] where the A_C and A_R are the areas of the heater condenser and the reboilers, respectively; L is the length of the vessel; D is the inside diameter of the column.

The design variables including the total stages (N_{T1}), fresh feed tray location (N_{F1}), and entrainer stream feeding location (N_{FE}) of the extractive distillation column, total stages (N_{T2}), and fresh tray location (N_{F2}) of the entrainer recovery column, are optimized to minimize TAC for the extractive distillation system. To facilitate the optimization, a calculation sequence is carefully established when there are so many variables. Such a sequential iterative optimization procedure is clearly demonstrated in Figure 6.

Figure 7a shows the TAC plot at various S/F ratios, it is observed that the optimum S/F ratio is 1. Figure 7b shows the results for varying N_{T1} with S/F ratio fixed at 1. It is concluded that the optimal N_{T1} is 66 with optimum N_{FE} and N_{F1}. Figure 7c shows the TAC plot at various N_{T2} with S/F ratios fixed at 1 and

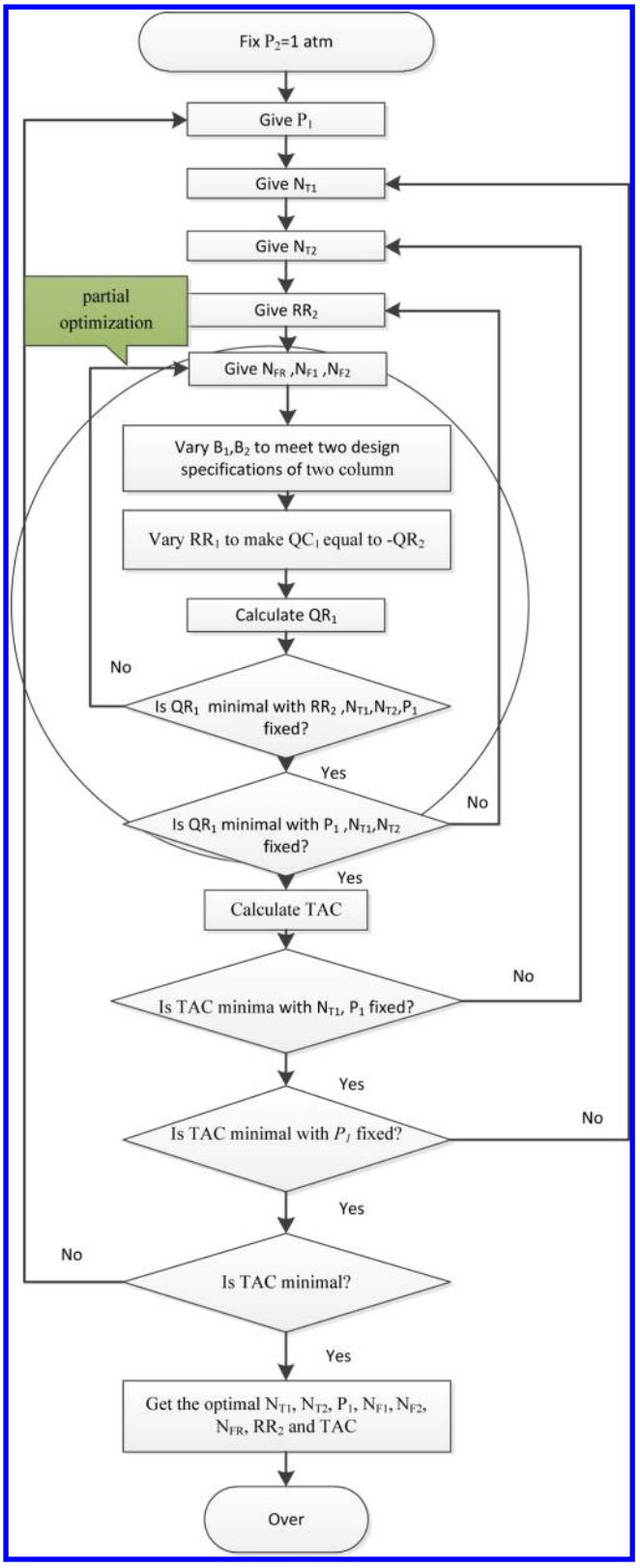

Figure 12. Sequential iterative optimization procedure for the fully heat-integrated pressure-swing distillation system.

N_{T1} fixed at 66, it is observed that the optimum N_{T2} is 40 with optimum N_{F2}. The economic optimal flowsheet is attained; the optimal design is $N_{T1} = 66$ and $N_{T2} = 40$, since it has the lowest TAC ($\$1.9638 \times 10^6$/annum) of all cases.

dx.doi.org/10.1021/ie502735g | Ind. Eng. Chem. Res. 2014, 53, 15167−15182

Table 5. Case Studies for Fully Heat-Integrated Pressure-Swing Distillation Process with HPC at 10 atm

parameters	case 1	case 2	case 3	case 4	case 5	case 6
N_{T1}	38	38	38	40	36	34
N_{T2}	16	18	20	18	18	18
ID_1 (m)	1.81	1.8	1.794	1.79	1.807	1.82
ID_2 (m)	1.52	1.51	1.50	1.50	1.517	1.53
QR_1 (kW)	2813.6	2785.8	2767.4	2767.4	2808.6	2839
QR_2 (kW)	1354.5	1299.4	1285.2	1285.5	1316.3	1299.9
TAC (10^6/annum)	1.856091	**1.85091**	1.8515	1.85317	1.850934	1.85424

Table 6. Case Studies for Fully Heat-Integrated Pressure-Swing Distillation Process with HPC at 12 atm

parameters	case 1	case 2	case 3	case 4	case 5	case 6
N_{T1}	36	36	36	40	38	34
N_{T2}	16	18	20	18	18	18
ID_1 (m)	1.825	1.816	1.81	1.8	1.808	1.829
ID_2 (m)	1.43	1.42	1.415	1.404	1.413	1.438
QR_1 (kW)	2669.98	2645.54	2629.34	2600.5	2620.82	2680.7
QR_2 (kW)	1086.5	1030.1	1018.37	1036.5	1050.88	1092.9
TAC (10^6/annum)	1.8698	**1.8648**	1.86554	1.86435	1.86385	1.87391

Table 7. Case Studies for Fully Heat-Integrated Pressure-Swing Distillation Process with HPC at 8 atm

parameters	case 1	case 2	case 3	case 4	case 5	case 6
N_{T1}	38	38	38	40	36	34
N_{T2}	18	20	22	20	20	20
ID_1 (m)	1.82	1.815	1.81	1.809	1.821	1.83
ID_2 (m)	1.626	1.619	1.614	1.612	1.627	1.638
QR_1 (kW)	3018.24	2995.3	2978.9	2977.2	3016.26	3045.64
QR_2 (kW)	1631.1	1612.8	1599.74	1598.48	1629.27	1652.19
TAC (10^6/annum)	1.93465	**1.93402**	1.93676	1.93689	1.93257	1.93565

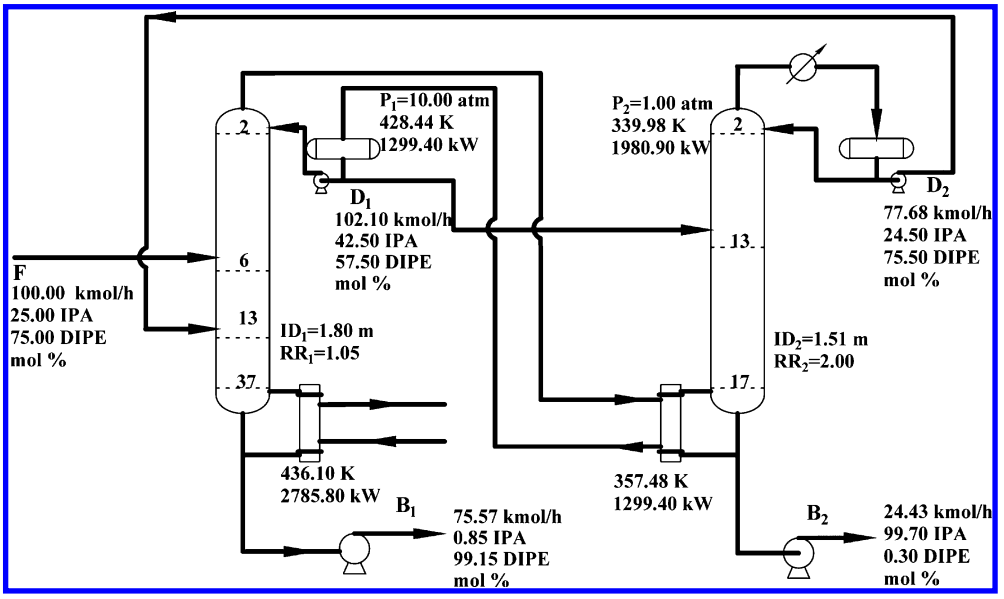

Figure 13. Optimal flowsheet for fully heat-integrated pressure-swing distillation system.

Figure 8 gives the optimal flowsheet for the conventional extractive distillation system with detailed equipment sizes, steam information, heat duties, and operating conditions at the steady-state design conditions.

2.1.4. Partially Heat-Integrated Extractive Distillation. During the past decades, great efforts have been made to improve energy utilization efficiency of the distillation process. As known from pressure-swing distillation, two columns are operated at different pressures, and it is possible to reduce energy consumption substantially by heat integration. This method can also be used in extractive distillation.

To achieve heat integration, an auxiliary reboiler is added to the extractive distillation process. For the sake of achieving the minimum heat transfer temperature difference, the pressure of entrainer recovery column should be raised to a pressure of 6 atm more. Thereby the overhead vapor can partially provide the

dx.doi.org/10.1021/ie502735g | Ind. Eng. Chem. Res. 2014, 53, 15167−15182

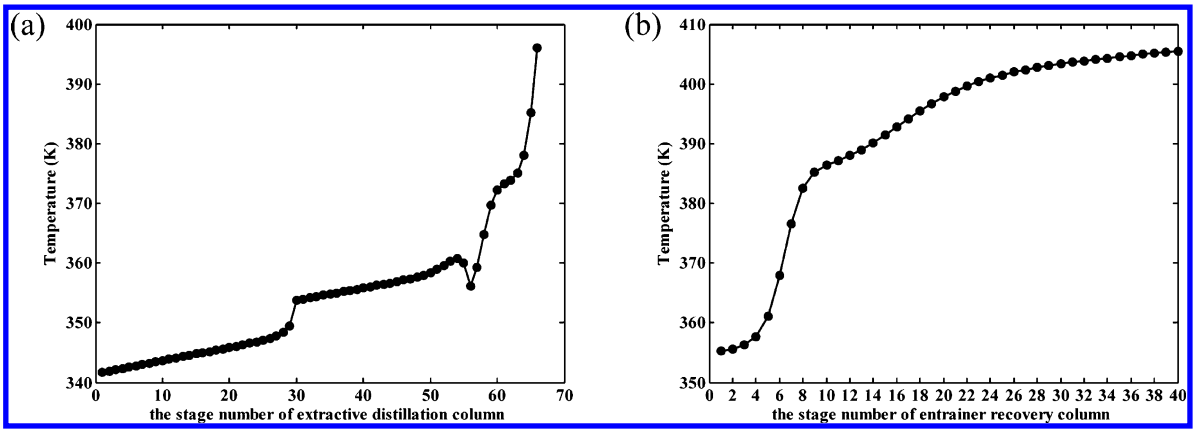

Figure 14. (a) Extractive distillation column and (b) entrainer recovery column temperature profile.

reboiler duty with the extractive distillation column. And the four design specifications remain the same with the conventional extraction distillation system.

The influence of pressure of entrainer recovery column on the TAC has been investigated with the plate number of two columns fixed. As P_2 is increased from 6 to 7 atm, it is revealed in the simulated results that TAC increases slightly, from \$2.149 × 10^6/annum to \$2.259 × 10^6/annum. But as P_2 is increased from 7 to 8 atm, TAC increases greatly up to \$2.745 × 10^6/annum. It is reasonable that P_2 is fixed at 6 atm. The effect of N_{T1} and N_{T2} on the TAC is shown in Figure 9. It is concluded that the optimal design with the lowest TAC (\$2.149 × 10^6/annum) is N_{T1} = 66 and N_{T2} = 56.

From Figure 10 the final optimal flowsheet for the partially heat-integrated extractive distillation system is given, with detailed equipment sizes, steam information, heat duties, and operating conditions at the steady-state design conditions.

By comparing the two optimal extraction distillation configurations, it is revealed that the conventional extractive distillation is more competitive than the partially heat-integrated extractive distillation from the economical viewpoint. For partially heat-integrated extractive distillation, although heat integration saves a large amount of energy, it does not effectively reduce the investment cost. The optimal design for the extractive distillation systems is N_{T1} = 66 and N_{T2} = 40, since it has the lowest TAC (\$1.964 × 10^6/annum) of all cases.

2.2. Pressure-Swing Distillation. The effect of pressure on the azeotropic composition of the DIPE/IPA is shown in Figure 11. It is clearly shown that changes in pressure significantly shift the composition of the azeotrope, and thus pressure-swing distillation can be applied to separate this binary mixture.

2.2.1. Steady State Design and Economical Optimization. To permit the use of cooling water with a temperature of around 305.15 K at the overhead, the operating pressure of the low-pressure column (LPC) is fixed at 1 atm. For the high-pressure column (HPC), the operating pressure should ensure 5 mol % or more change in the azeotrope composition over an appropriate range of pressure.[34] And in the following part of this paper, the operating pressure of the high-pressure column will be optimized from an economical view.

Before the steady-state simulation, the number of theoretical trays is selected, 40 trays for the LPC and 22 for the HPC. Initial estimate values for the reflux ratio of the LPC and HPC are 2.2 and 1.5, respectively. The recycled stream and feed stream are fed to the middle of HPC, and the feed stage of LPC is exactly at the middle of the column too. The operating pressure of the HPC is fixed at 10 atm. Figure 3 gives the $T-x,y$ curves for a DIPE/IPA binary mixture at 1 and 10 atm. It is known from the result of the simulation, the reboiler and condenser duties are 1263.85 kW and 1930.3 kW for the LPC, respectively, and the reboiler and condenser duties are 3029.77 kW and 1556.82 kW for the HPC, respectively. The temperature of the LPC reboiler and the HPC condenser are 358.43 and 428.47 K, respectively. This indicates that there is the possibility of heat integration between the two columns, which could decrease operating costs and fixed capital investment by a large margin.

In this section, full heat integration is considered so that neat operation can be achieved without an auxiliary reboiler or condenser. The "RadFrac" block in Aspen Plus is used to implement rigorous distillation simulation. These runs are made with the distillate and bottoms compositions held at their specified values. In the HPC, the bottoms composition specification is 99.5 wt % DIPE. In the LPC, the bottoms composition specification is 99.5 wt % IPA. The "flowsheet design spec" function is used to maintain the reboiler duty of LPC and is exactly equal to the condenser duty of HPC; therefore the full heat integration between the two columns can be achieved.

Increasing the operating pressure of HPC significantly shifts the composition of the azeotrope, which further reduces the recycle flow rate and energy consumption. The higher is the operating pressure of the HPC, the lower is the temperature difference between the steam and the HPC reboiler; a larger heat transfer area is required, which leads to an increase in the fixed capital investment. A trade-off between the operating costs and the fixed capital costs should be considered. Therefore, an appropriate operating pressure must be selected.

A number of design variables should be determined: the total stages (N_{T1}), fresh feed tray location (N_{F1}) of the HPC, total stages (N_{T2}), fresh tray location (N_{F2}) of LPC, the recycle feed tray location (N_{FR}), the operating pressures of HPC and the LPC reflux ratio (RR_2). Because so many design variables need to be optimized, a calculation sequence is carefully established to facilitate the optimization. Such a sequential iterative optimization procedure is clearly demonstrated in Figure 12.

Tables 5−7 give the details of each case and the TACs with the HPC operating pressures at 8, 10, and 12 atm, respectively. It is noticed that the effect of HPC operating pressure on the TAC is surprisingly bigger compared to the effect of the number of theoretical plates. This suggests that selecting an appropriate operating pressure is more important than picking the number of theoretical plates for this process. It is observed that the optimum

dx.doi.org/10.1021/ie502735g | Ind. Eng. Chem. Res. 2014, 53, 15167−15182

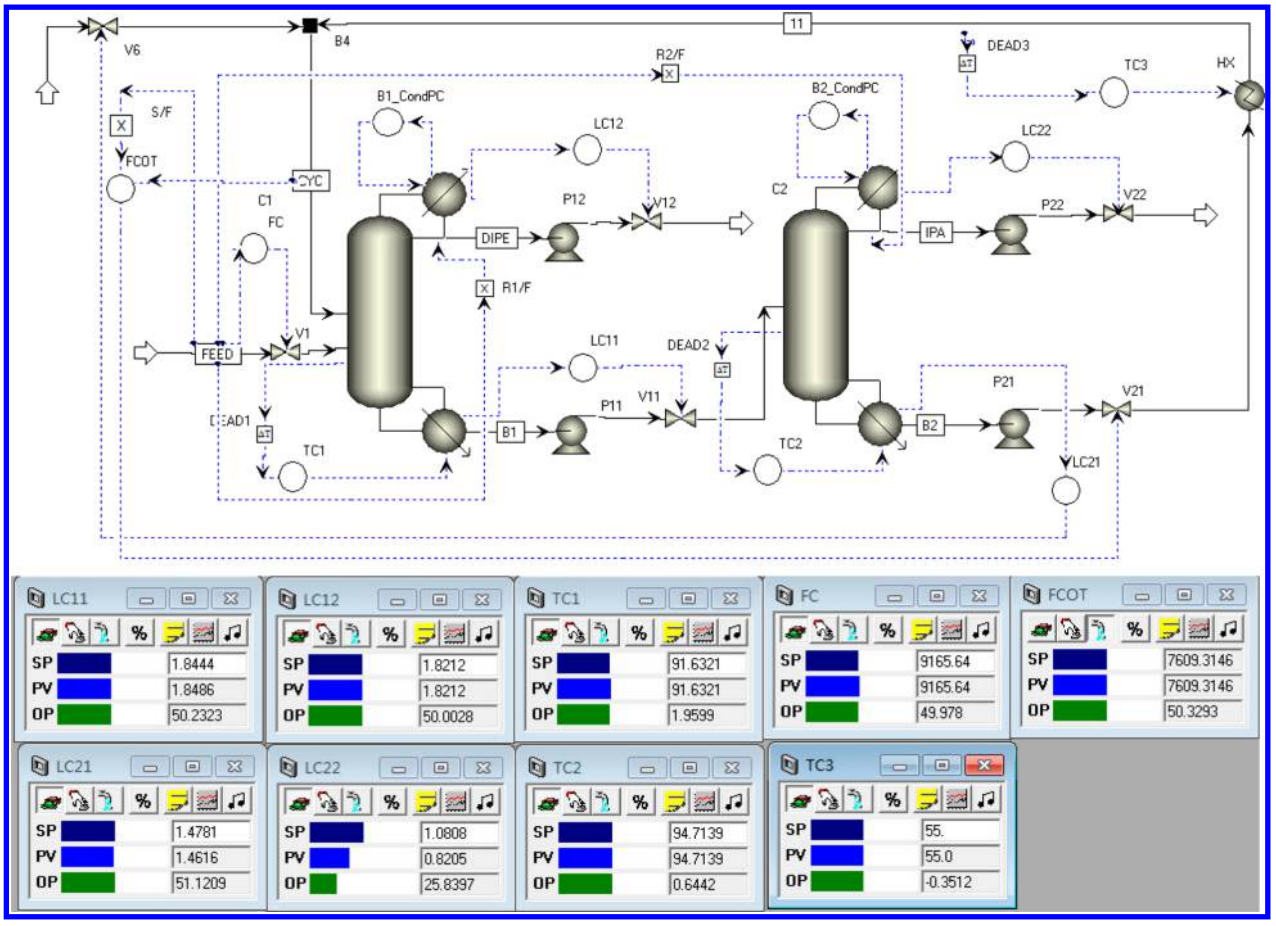

Figure 15. Control structures for the extractive distillation system.

for this pressure-swing distillation process corresponds to case 2 in Table 5, with an HPC at 10 atm.

Figure 13 gives the fully heat-integrated flowsheet with detailed equipment sizes, steam information, heat duties, and operating conditions at the steady state design conditions. This corresponds to case 2 from Table 5 with HPC at 10 atm.

3. CONTROL SYSTEM DESIGN

Apart from the economic benefit of a distillation process, the performance of dynamic control is another important factor. It is of importance to study the controllability of the two processes. Before starting the dynamic simulation, the major equipment sizes and plumbing system must be specified. The commonly used heuristic for column bases sizing and reflux drums is to provide 10 min of holdup when full, using the total liquid entering or leaving these locations. Most valves' pressure drops are 3 atm with the valve half open at the design flow rate. Then the steady state flowsheet is pressure checked, and the Aspen Plus file is exported to Aspen Dynamics.

Table 8. Temperature Controllers Tuning Parameters for Extractive Distillation Column

parameters	TC1	TC2	TC3
controlled variable	$T_{1,56}$	$T_{2,6}$	$T_{recycle}$
manipulated variable	QR_1	QR_2	Q_{HX}
gain, K_c	1.720	0.910	0.260
integral time, τ_I (min)	11.900	17.200	5.300

3.1. Extractive Distillation in Dynamic Simulation. One control strategy is developed for the optimal design of the extractive distillation systems. Figure 14 gives the temperature profiles of the two columns. It is noticed that stage 58 displays a fairly steep slope for the extractive distillation column, and stage 6, for the entrainer recovery column. These indicate the proper temperature control point for the two columns. The basic control structure for this two-column system is shown in Figure 15. The detailed control structures are outlined as below:

(1) The operating pressure in the two columns is controlled by manipulating the heat removal rate in the condenser of the two columns (reverse acting).
(2) Entrainer feed temperature is held by manipulating the cooler HX heat duty (reverse acting).
(3) The total entrainer flow rate is in proportion to the fresh feed flow rate.
(4) Base level in the entrainer recovery distillation column is held by manipulating the makeup 2-MEA flow rate (reverse acting).
(5) Base level in the extractive distillation column is held by manipulating the flow of the bottoms (direct acting).
(6) The temperature for stage 58 in the extractive distillation column is controlled by manipulating the reboiler heat input into the extractive distillation column (reverse acting).
(7) The temperature for stage 6 in the entrainer recovery column is controlled by manipulating the reboiler heat input into the entrainer recovery column (direct acting).

dx.doi.org/10.1021/ie502735g | Ind. Eng. Chem. Res. 2014, 53, 15167−15182

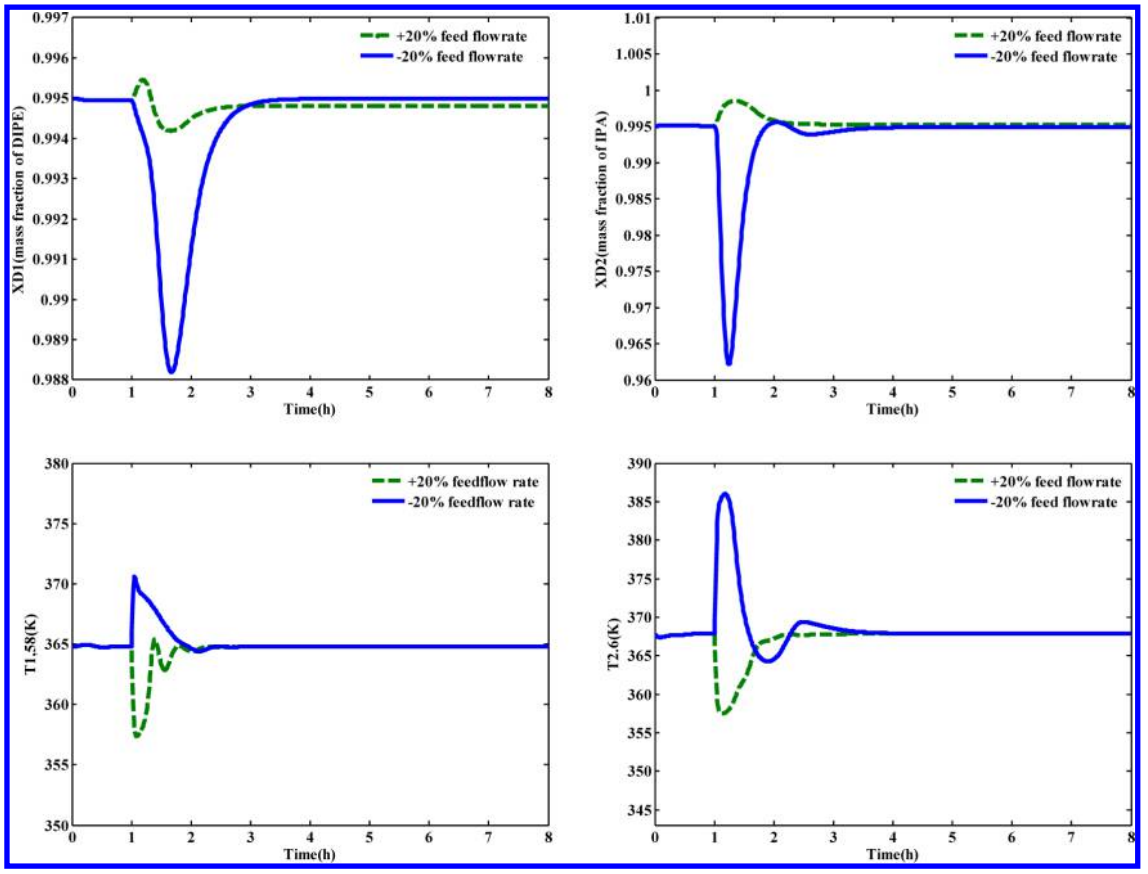

Figure 16. Dynamic responses for control structures: feed flow rate disturbances.

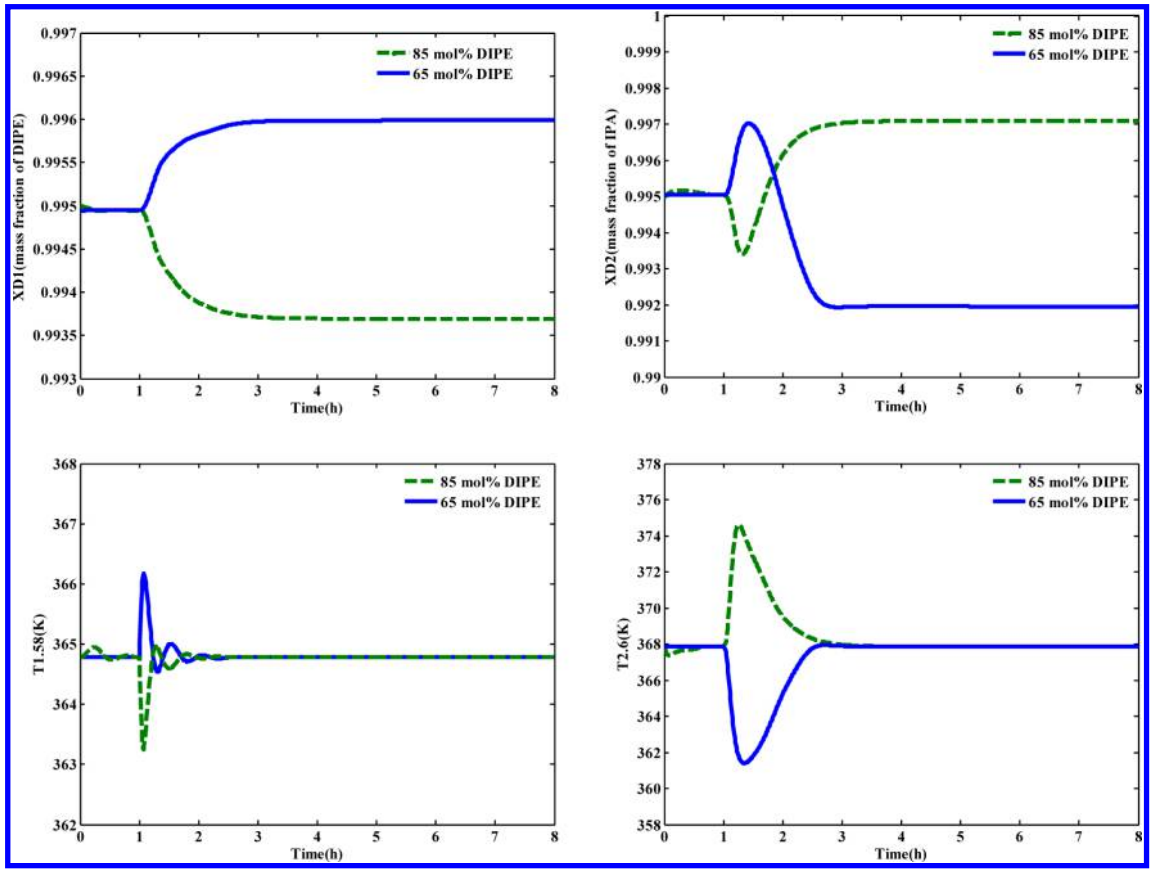

Figure 17. Dynamic responses for control structures: feed composition disturbances.

dx.doi.org/10.1021/ie502735g | *Ind. Eng. Chem. Res.* 2014, 53, 15167−15182

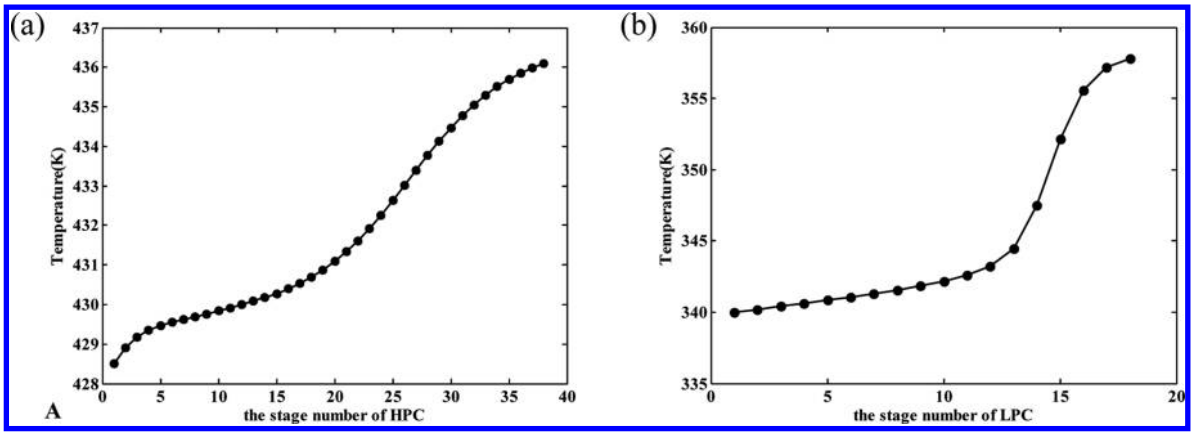

Figure 18. Temperature profiles of (a) HPC and , (b) LPC in the distillation system.

Table 9. Temperature Controllers Tuning Parameters for Fully Heat-Integrated Pressure-Swing Distillation

parameters	TC1	TC2
controlled variable	T_{PC}	$T_{1.28}$
manipulated variable	QR_2	RR_1
gain,K_c	7.250	1.030
integral time, τ_I (min)	9.240	19.800

(8) Reflux drum levels in both columns are held by manipulating the flow of distillates (direct acting).
(9) Feed is flow-controlled (reverse acting).
(10) The reflux flow rate of two columns is in proportion to the fresh feed flow rate.

Proportional-only controllers are used for all liquid levels with K_c = 2. The proportional and integral (PI) settings of the top pressure control loops for both columns are set at K_c = 20 and τ_I = 12 min. Three deadtime elements are inserted into the corresponding temperature control loops with a deadtime of 1 min. Relay-feedback tests are run on the three temperature controllers to determine ultimate gains and periods, and Tyreus−Luyben tuning is used in the three controllers. Table 8 gives the three temperature controller parameters.

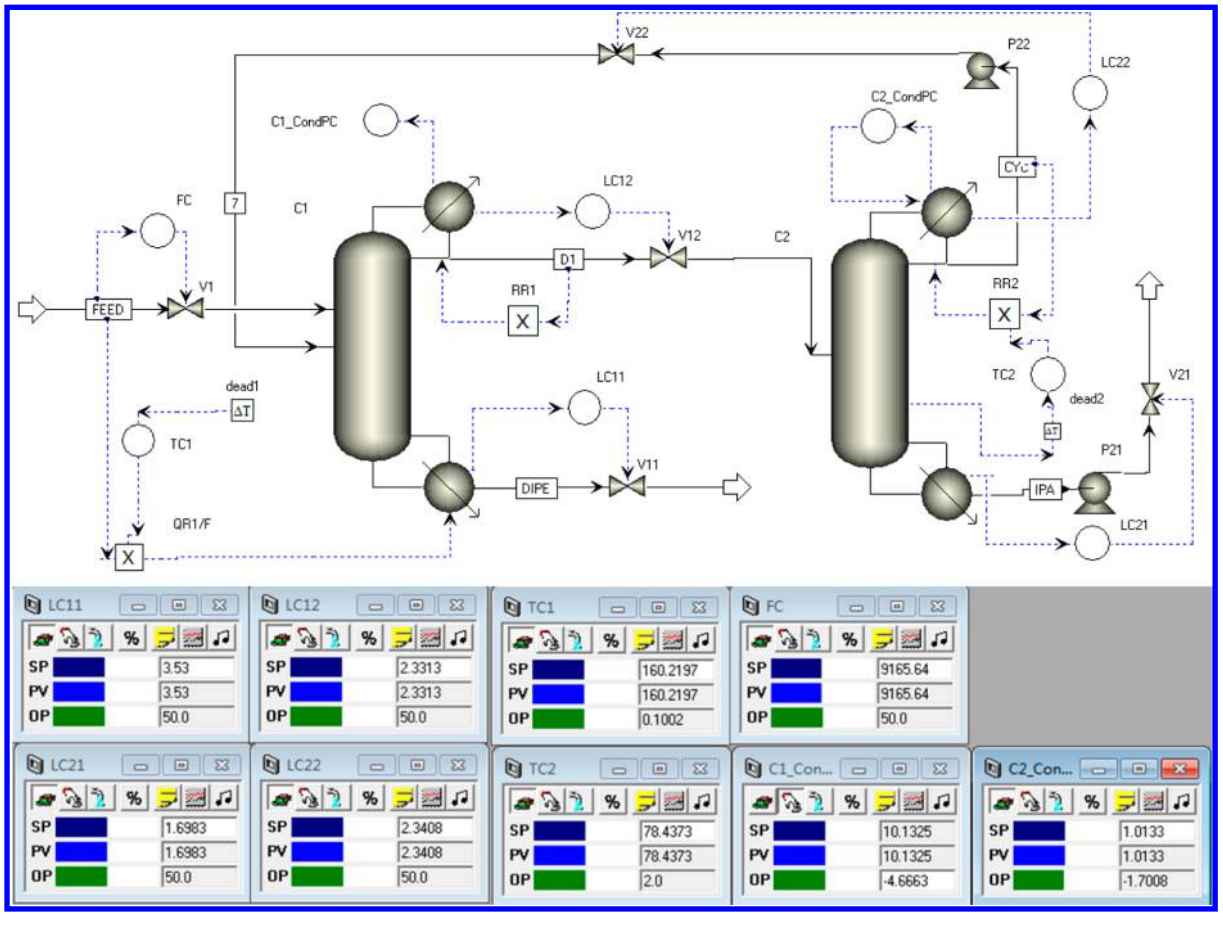

Figure 19. Control structures for the fully heat-integrated pressure swing distillation system.

dx.doi.org/10.1021/ie502735g | Ind. Eng. Chem. Res. 2014, 53, 15167−15182

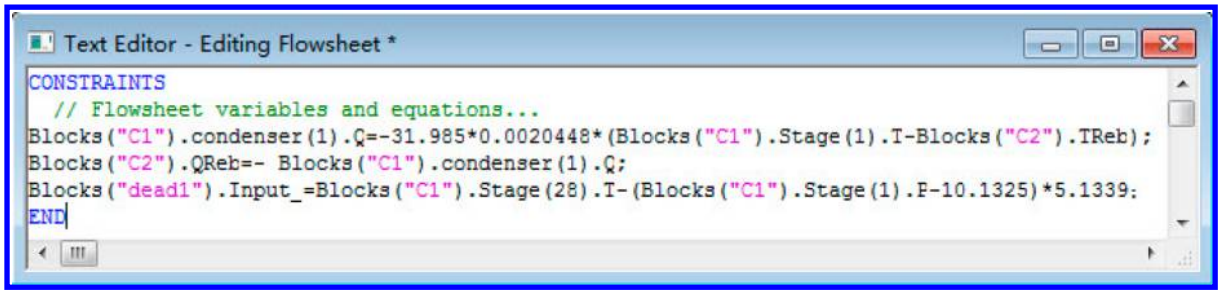

Figure 20. Flowsheet equations for fully heat-integrated pressure-swing distillation by using pressure-compensated temperature control.

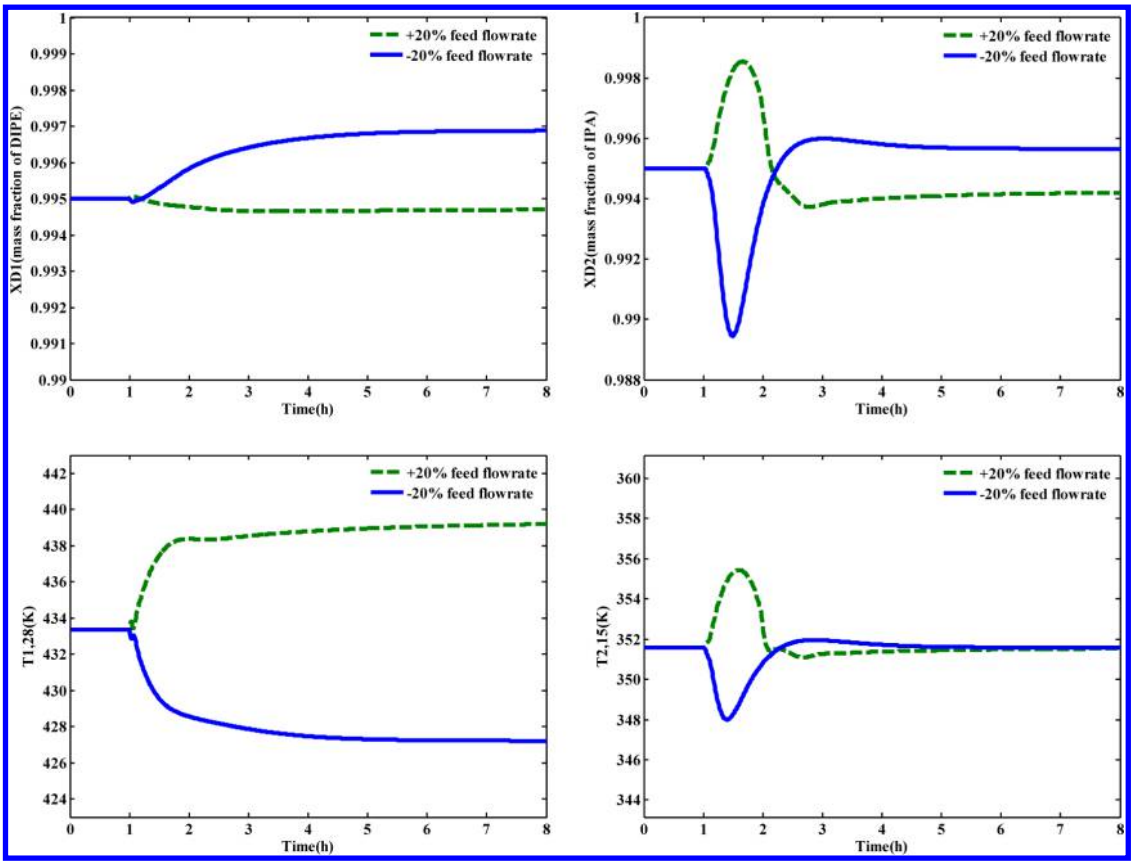

Figure 21. Dynamic responses for control structure: 20% feed flow rate disturbances.

Feed flow rate and composition disturbances are introduced into the system to evaluate the dynamic performance of this control structure. The dynamic responses of this control structure to 20% increase and decrease in feed flow rate are shown in Figure 16. Feed flow rate disturbances are introduced into the system at 1 h. It is noticed that product purities are held fairly close to their desired values at the new steady state about 3 h, and the two controlled tray temperatures are brought back to their set points. The dynamic responses of this control structure to feed composition disturbances are shown in Figure 17. Feed composition disturbances are introduced into the system at 1 h, too. It is noticed that product purities are held fairly close to their desired values at the new steady state about 3 h, and the two controlled tray temperatures are brought back to their set points.

3.2. Fully Heat-Integrated Pressure-Swing Distillation in Dynamic Simulation. In this section, the optimal design of a fully heat-integrated pressure-swing distillation system is considered only for control system design. The plumbing system and major equipment sizes are specified according to the criteria mentioned in section 3.1. As seen from Figure 18, stage 15 displays a fairly steep slope for LPC, as does stage 28 for HPC. These indicate the proper temperature control point for the two columns.

The proportional-integral controllers are tuned by running a relay-feedback test with the use of the Tyreus−Luyben settings. Table 9 gives the two temperature controller parameters. On account of the two columns which are fully heat-integrated, the "flowsheet equations" function is used to achieve full heat integration in Aspen Dynamics. Figure 20 shows the appropriate equations entered in the editor window. The two variables that must be changed from *Fixed* to *Free* are the heat duty in the condenser of the high-pressure column and the heat duty in the reboiler of the low-pressure column.

The basic control structures for the fully heat-integrated pressure-swing distillation system are shown in Figure 19. The detailed control structures are outlined as below:

(1) The reflux ratio in the high-pressure column is fixed.

dx.doi.org/10.1021/ie502735g | *Ind. Eng. Chem. Res.* 2014, 53, 15167−15182

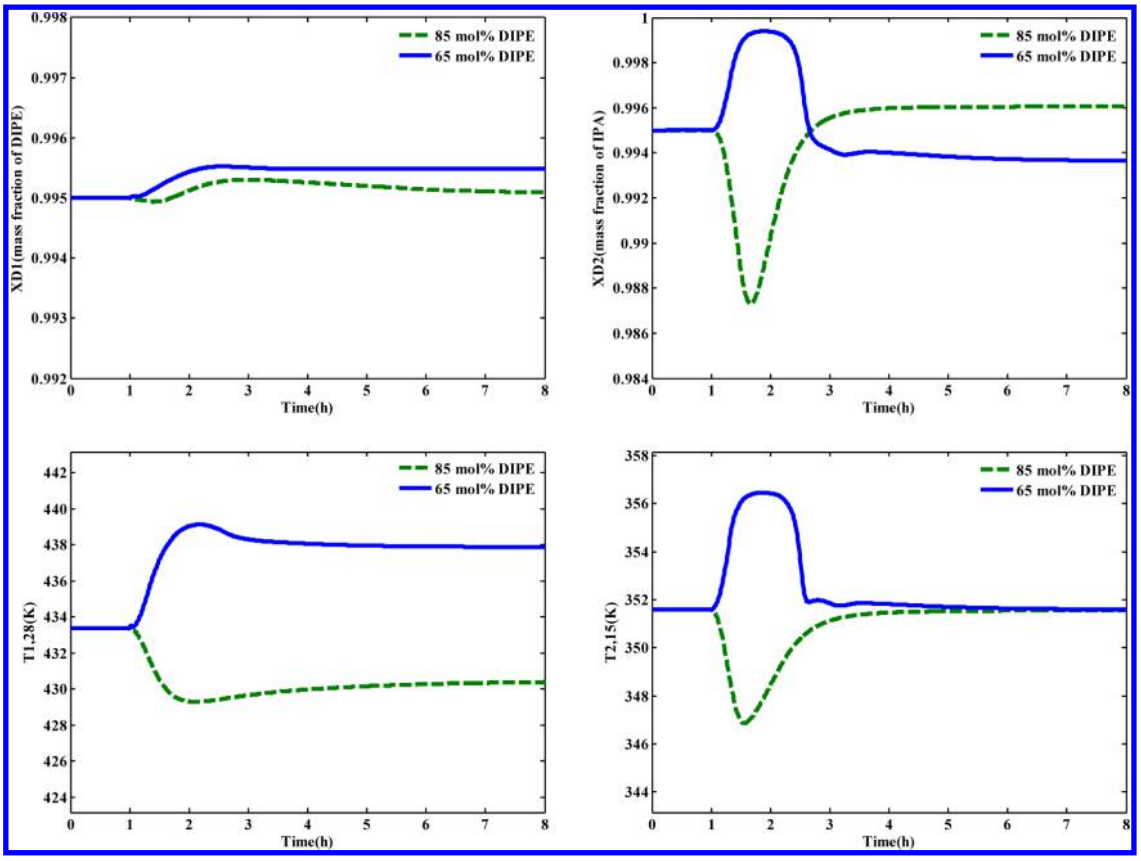

Figure 22. Dynamic responses for control structure: feed composition disturbances.

(2) The operating pressure in the low-pressure column is controlled by manipulating the heat removal rate in the condenser of the low-pressure column (reverse acting).
(3) The temperature for stage 15 in the low-pressure column is controlled by manipulating the reflux ratio in the low-pressure column (direct acting).
(4) Base levels in both columns are held by manipulating the corresponding bottoms flow rate (direct acting).
(5) Reflux drum levels in both columns are held by the corresponding manipulating distillates flow rate (direct acting).
(6) Feed is flow-controlled (reverse acting).
(7) The operating pressure in the high-pressure column is manual controlled.

The operating pressure in the high-pressure column is floated with the operating conditions by setting pressure control on manual; a pressure-compensated temperature control scheme should be added. The top pressure and the temperature for stage 28 in the high-pressure column are measured. Liquid composition for stage 28 in the high-pressure column is 5.98/94.02 wt % DIPE/IPA. The bubble point of the DIPE/IPA mixture is varied linearly with pressure (8—12 atm), with a slope of 5.1339 K/bar. The "Flowsheet Equations" function in Aspen Dynamics is employed to achieve the pressure-compensated temperature control, as shown in Figure 20.

As observed from Figures 21 and 22, this control scheme can handle both feed flow rate and feed composition disturbances well, with only small offsets in the product purities at the new steady states.

4. PROCESS COMPARISONS

In this section, we will make a comparison between extractive distillation and fully heat-integrated pressure-swing distillation systems in terms of steady-state economics and dynamic controllability. The optimal configurations of the two methods have been attained by using the same criteria and evaluation procedures. The optimal results are shown in Table 10. For the DIPE/IPA separation, the fully heat-integrated pressure-swing distillation conserves 7.97% energy consumption and reduces 5.75% TAC compared with extractive distillation. Although the fully heat-integrated pressure-swing distillation offers 7.97% saving in energy consumption, the reduction margin of TAC (5.75%) is smaller than this value. This is mainly because in the pressure-swing distillation process, one column is operating at high pressure, which means that a thicker vessel wall is required for the HPC vessel and heat exchangers. In addition, the price of the heating steam of HPC is higher than the extractive distillation system.

Table 10. Optimal Results for Extractive Distillation and Fully Heat-Integrated Pressure-Swing Distillation Systems

parameters	extractive distillation	pressure-swing distillation
N_{T1}	66	38
N_{T2}	40	18
QR_1 (kW)	2279.45	2785.8
QR_2 (kW)	747.626	1299.4
TAC ($\$10^6$/annum)	1.964	**1.851**

Control structures are also developed for the two methods. The dynamic performances of fully heat-integrated pressure

dx.doi.org/10.1021/ie502735g | Ind. Eng. Chem. Res. 2014, 53, 15167−15182

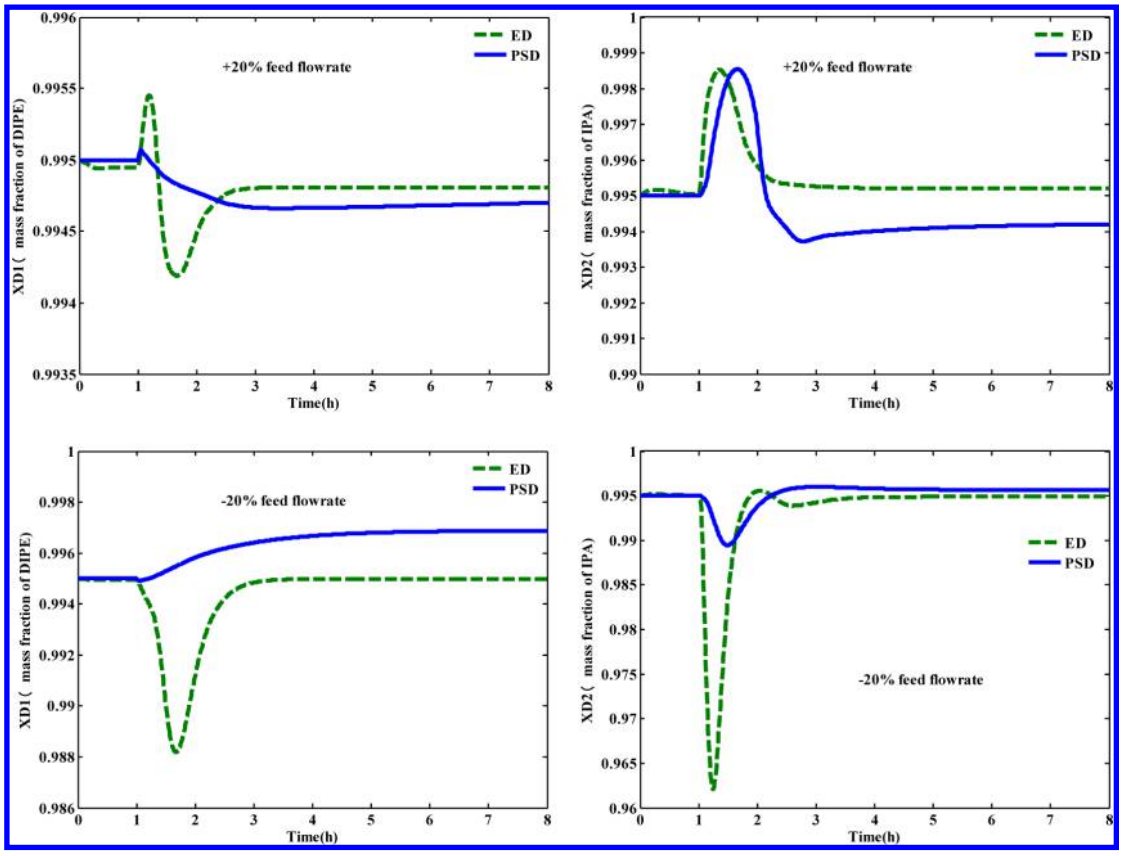

Figure 23. Comparisons of dynamic performance between presure-swing distillation and extractive distillation for feed flow rate disturbances.

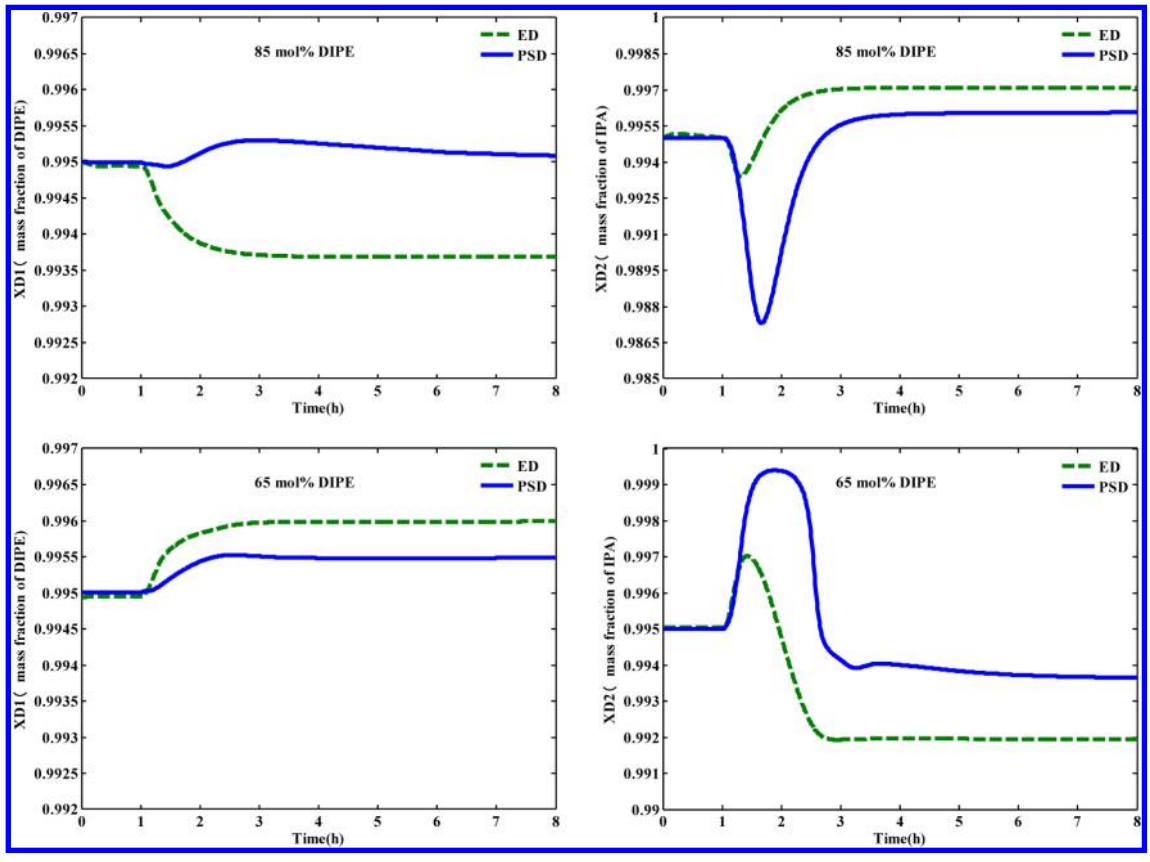

Figure 24. Comparisons of dynamic performance between presure-swing distillation and extractive distillation for feed composition disturbances.

dx.doi.org/10.1021/ie502735g | *Ind. Eng. Chem. Res.* 2014, 53, 15167−15182

swing distillation system and extractive distillation system are compared. Figures 23 and 24 give a direct dynamic comparison of the two alternatives for the same feed flow rate and feed composition disturbances. It is observed that two distillation processes maintain both products purity at acceptable levels of quality in 3 h after several oscillations.

As seen from Figure 23, the extractive distillation process has larger transient deviations in maintaining the DIPE product purity when ±20% feed flow rate disturbances are introduced. It is noticed that the two process have similar transient deviations in maintaining the IPA product purity when +20% feed flow rate disturbance is introduced, whereas the extractive distillation process has larger transient deviations in maintaining the IPA product purity when a −20% feed flow rate disturbance is introduced. As shown in Figure 24, the fully heat-integrated pressure-swing distillation process has smaller transient deviations in maintaining the DIPE product purity when feed composition disturbances are introduced; in contrast, the extractive distillation process has smaller transient deviations in maintaining the IPA purity.

5. CONCLUSIONS

Two methods for separating diisopropyl ether and isopropyl alcohol azeotropic mixtures are investigated: extractive distillation and fully heat-integrated pressure-swing distillation. Using a criterion for entrainer selection, 2-methoxyethanol is selected as a suitable entrainer. On the basis of the proposed optimization method with total annual cost as the objective function, the optimal design of the extractive distillation process is attained with the optimal total stages of 66 for the extractive distillation column, 40 for the entrainer recovery distillation column and two columns working at 1 atm. The fully heat-integrated pressure-swing distillation system is explored, using a proposed optimization method. It is revealed that a high-pressure column working at 10 atm is reasonable, and the optimal total number of stages is 38 for the high-pressure column and 18 for the low-pressure column. The pressure-swing distillation process has reduced the total annual cost and energy consumption versus the extractive distillation process by 5.75% and 7.97%, respectively. It is concluded that the fully heat-integrated pressure-swing distillation process is more attractive in terms of steady-state economics.

Two control structures are proposed for the optimal extractive distillation and fully heat-integrated pressure-swing distillation configurations, respectively. The extractive distillation process shows better controllability in maintaining the two products' purity for feed flow rate disturbances, whereas the fully heat-integrated pressure-swing distillation process shows better controllability in maintaining the purity of the two products for feed composition disturbances. It is noticed that both processes can be applied to the diisopropyl ether/isopropyl alcohol separation from the standpoint of dynamic control stability.

AUTHOR INFORMATION

Corresponding Author

*Tel: +86 022-27892145. Fax: +86 022-27404440. E-mail: cjxu@tju.edu.cn.

Notes

The authors declare no competing financial interest.

ACKNOWLEDGMENTS

The authors thank the Programme of Introducing Talents of Discipline to Universities (No: B06006) for support and the staff in the State Key Laboratories of Chemical Engineering (Tianjin University) for assistance.

NOMENCLATURE

DIPE = diisopropyl ether
IPA = isopropyl alcohol
2-MEA = 2-methoxyethanol
TAME = tert-amyl methyl ether
RCM = residue curve map
TAC = total annual cost
ED = extractive distillation
PSD = pressure-swing distillation
HPC = high-pressure column
LPC = low-pressure column
$\alpha_{i,j}$ = separation factor of components i and j
NRTL = nonrandom two liquid
N_{FE} = feeding location for the entrainer
N_{FR} = feeding location for recycle stream
N_{Fn} = feeding location for column n
N_{Tn} = number of theoretical plates for column n
B_n = bottom flow rate from column n (kmol/h)
D_n = bottom flow rate from column n (kmol/h)
ID_n = internal diameter for column n (m)
P_n = top pressure of column n (atm)
QC_n = condenser heat removal for column n (kW)
QR_n = reboiler heat input for column n (kW)
RR_n = reflux ratio for column n

REFERENCES

(1) Wang, S. J.; Wong David, S. H.; Yu, S. W. Effect of Entrainer Loss on Plant-Wide Design and Control of an Isopropanol Dehydration Process. *Ind. Eng. Chem. Res.* **2008**, *47* (17), 6672−6684.
(2) Logsdon, J. E.; Loke, R. A. Isopropyl alcohol. *Kirk−Othmer Encyclopedia of Chemical Technology*; Wiley: New York, 2000
(3) Seader, J. D.; Henley, E. J. *Separation Process Principles*; John Wiley & Sons: New York, 1998; p 604.
(4) Lei, Z. G.; Li, C. Y.; Chen, B. H. Extractive Distillation: A review. *Sep. Purif. Technol. Rev.* **2003**, *32*, 121−213.
(5) Errico, M.; Rong, B. G.; Tola, G.; Spano, M. Optimal synthesis of distillation systems for bioethanol separation. Part 1: Extractive distillation with simple columns. *Ind. Eng. Chem. Res.* **2013**, *52*, 1612−1619.
(6) Errico, M.; Rong, B. G.; Tola, G.; Spano, M. Optimal synthesis of distillation systems for bioethanol separation. Part 2: Extractive distillation with complex columns. *Ind. Eng. Chem. Res.* **2013**, *52*, 1620−1626.
(7) Liang, K.; Li, W.; Luo, H.; Xia, M.; Xu, C. Energy-Efficient Extractive Distillation Process by Combining Preconcentration Column and Entrainer Recovery Column. *Ind. Eng. Chem. Res.* **2014**, *53*, 7121−7131.
(8) Kissack, S.; Kraemer, K.; Gani, R.; Marquardt, W. A systematic synthesis framework for extractive distillation processes. *Chem. Eng. Res. Des.* **2008**, *86*, 781−792.
(9) Lang, P.; Modla, G.; Benadda, G.; Lelkes, Z. Homoazeotropic distillation of maximum azeotropes in a batch rectifier with continuous entrainer feeding I. Feasibility studies. *Com. Chem. Eng.* **2000**, *24*, 1665−1671.
(10) Lang, P.; Modla, G.; Kotai, B.; Lelkes, Z.; Moszkowicz, P. Homoazeotropic distillation of maximum azeotropes in a batch rectifier with continuous entrainer feeding II. Rigorous simulation results. *Com. Chem. Eng.* **2000**, *24*, 1429−1435.

(11) Lei, Z.; Wang, H.; Zhou, R. Influence of salt added to solvent on extractive distillation. *Chem. Eng. J.* **2002**, *87*, 149−156.
(12) Arifin, S.; Chien, I. L. Combined preconcentrator/recovery column design for isopropyl alcohol dehydration process. *Ind. Eng. Chem. Res.* **2007**, *46*, 2535.
(13) Wang, Q.; Yu, B.; Xu, C. Design and control of distillation system for methylal/methanol separation. Part 1: Extractive distillation using DMF as an entrainer. *Ind. Eng. Chem. Res.* **2012**, *51*, 1281−1292.
(14) Knapp, J. P.; Doherty, M. F. Thermal integration of homogeneous azeotropic distillation sequences. *AIChE J.* **1990**, *36*, 969−984.
(15) Lewis W. K. Dehydrating alcohol and the like. US Patent, 1,676,700, July 10, 1928.
(16) Müller, W. H. E.; Kaufhold, M. Process for the recovery of pure methylal from methanol-methylal mixtures. U.S. Patent 4,385,965, May31, 1983.
(17) Muñoz, R.; Montón, J. B.; Burguet, M. C.; Torre, J.; de la. Separation of isobutyl alcohol and isobutyl acetate by extractive distillation and pressure-swing distillation: simulation and optimization. *Sep. Purif. Technol.* **2006**, *50*, 175−183.
(18) Luyben, W. L. Comparison of extractive distillation and pressure-swing distillation for acetone-methanol separation. *Ind. Eng. Chem. Res.* **2008**, *47*, 2696−2707.
(19) Skogestad, S. Dynamic and control of distillation columns: A critical survey. *Model. Ident. Control* **1997**, *18*, 177−217.
(20) Luyben, W. L. Sensitivity of distillation relative gain arrays to steady-state gains. *Ind. Eng. Chem. Res.* **1987**, *26*, 2076−2078.
(21) Luyben, W. L. Comparison of pressure-swing and extractive distillation methods for methanol-recovery system in the TAME reactive-distillation process. *Ind. Eng. Chem. Res.* **2005**, *44*, 5715−5725.
(22) Yu, B.; Wang, Q.; Xu, C. Design and control of distillation system for methylal/methanol separation. Part 2: Pressure swing distillation with full heat integration. *Ind. Eng. Chem. Res.* **2012**, *51*, 1293−1310.
(23) Modla, G.; Lang, P. Removal and recovery of organic solvents from aqueous waste mixtures by extractive and pressure swing distillation. *Ind. Eng. Chem. Res.* **2012**, *51*, 11473−11481.
(24) Lladosa, E.; Montón, J. B.; Cruz Burguet, M. Separation of di-*n*-propyl ether and *n*-propyl alcohol by extractive distillation and pressure swing distillation: computer simulation and economic optimization. *Chem. Eng. Proc.* **2011**, *50*, 1266−1274.
(25) Dyk, B. V.; Nieuwoudt, I. Design of solvents for extractive distillation. *Ind. Eng. Chem. Res.* **2000**, *39*, 1423−1429.
(26) Lladosa, E.; Monton, J. B.; Burguet, M.; Munoz, R. Isobaric vapor−liquid equilibria for binary and ternary mixtures of diisopropyl ether, 2-propyl alcohol, and 3-methyl-1-butanol. *J. Chem. Eng. Data* **2008**, *53*, 1897−1902.
(27) Lladosa, E.; Monton, J. B.; Burguet, M.; Munoz, R. Effect of pressure and the capability of 2-methoxyethanol as solvent in the behaviour of diisopropyl ether-isopropyl alcohol azeotropic mixture. *Fluid. Phase. Equilib.* **2007**, 271−279.
(28) ŠtepánPsutka, Ivan Wichterle. Isothermal vapour−liquid equilibria in the binary and ternary systems composed of 2-propanol, diisopropyl ether and 1-methoxy-2-propanol. *Fluid Phase Equilib.* **2004**, *220*, 161−165.
(29) Phama, H. N.; Doherty, M. F. Design and synthesis of heterogeneous azeotropic distillations—II. Residue curve maps. *Chem. Eng. Sci.* **1990**, *45*, 1837−1843.
(30) Doherty, M. F.; Caldarola, G. A. Design and synthesis of homogeneous azeotropic distillations. 3. The sequencing of columns for azeotropic and extractive distillations. *Ind. Eng. Chem. Fundam.* **1985**, *24*, 474−485.
(31) Luyben, W. L. *Distillation Design and Control Using Aspen Simulation*; John Wiley &Sons, Inc: New York, 2006.
(32) Knight, J. R.; Doherty, M. F. Optimal design and synthesis of homogeneous azeotropic distillation sequences. *Ind. Eng. Chem. Res.* **1989**, *28*, 564−572.
(33) Luyben, W. L. *Plantwide Dynamic Simulation in Chemical Processing and Control*; Marcel Dekker: New York, 2002.
(34) Seader, J. D.; Henley, E. J. *Separation process principles*; John Wiley & Sons, Inc.: Hoboken, NJ, 1998; pp 612.